In-situ observation of morphological change of Pd-based bimetallic nanoparticles synthesized by co-sputtering

N. Nakamura,[1, a)] K. Matsuura,[2] and A. Ishii[2]

[1)] *Graduate School of Engineering, Osaka University, 2-1 Yamadaoka, Suita, Osaka 565-0871, Japan*

[2)] *Graduate School of Engineering Science, Osaka University, 1-3 Machikaneyama, Toyonaka, Osaka 560-8531, Japan*

(Dated: 28 August 2023)

The formation process of Pd-based bimetallic nanoparticles synthesized by co-sputtering is investigated by performing the in-situ morphological observation using the resistive spectroscopy. The segregation of the metal with lower surface energy on the nanoparticle surface is observed, and it is found that the formation process of the alloy nanoparticles tends to be similar to that of the nanoparticles composed of the core metal even when the atomic fraction of the shell metal is higher than that of the core metal. The co-sputtering process is simulated by the molecular dynamics analysis, and the observed formation process is theoretically confirmed.

[a)] nakamura@mech.eng.osaka-u.ac.jp

I. INTRODUCTION

The unique properties of bimetallic nanoparticles, which differ from those of bulk materials and single-element nanoparticles, have attracted the interest of researchers, and their synthesis methods, properties, and applications have been investigated[1,2]. Since the properties change depending on their structure such as core-shell structures, mixed structures, intermetallic alloy structures, and so on., the preferred structures have been identified by simulations using the density function theory (DFT)[3], the equivalent-medium approximation and bond-strength modifications[4], and the Monte Carlo simulations with DFT-based embedded-atom potential[5]. However, the structures of experimentally synthesized nanoparticles sometimes differ from those simulated. For example, for PdAu nanoparticles, an Au-shell/Pd-core structure is expected to be preferable[3–5]. Such Au-shell/Pd-core structure has been observed in nanoparticles synthesized by the evaporation on silica[6], and it is also observed when Au is deposited first, followed by Pd on oxide surfaces[7]. In contrast, the Pd-shell/Au-core structure is observed in nanoparticles synthesized by the chemical deposition[8,9] and one-step aqueous synthesis[10]. Furthermore, a homogeneously alloyed structure is observed for nanoparticles synthesized by the simultaneous sputter deposition into an ionic liquid[11]. Thus, the preferred structure predicted by the simulations and that observed in the experiments are not necessarily in agreement, and the formation process and the preferred structure of the nanoparticles are not fully understood. This situation arises from the difficulty of real-time observation of the formation process and would be resolved if it is possible to observe in real time.

Structural characterization of bimetallic nanoparticles is performed using atomic force microscopy, scanning electron microscopy, transmission electron microscopy, X-ray photoelectron spectroscopy, X-ray diffraction, ultraviolet-visible spectroscopy and so on.[9,12–15], which are the post-characterization methods. In-situ characterization is performed during dewetting using the dynamic transmission electron microscope[16], but real-time structural characterization is hardly performed. Under these circumstances, we have developed a methodology, in which the formation process is monitored from the nanoparticle shape measured through the resonant vibration of a piezoelectric oscillator[17]. Using this method, in this study we investigate the formation process of Pd-based bimetallic nanoparticles synthesized by the co-sputtering. It is a feature of the co-sputtering that can control the composition by

changing the deposition rate of metals, and it has been used to form bimetallic nanoparticles on a solid surface[18,19] and in a liquid polymer[20]. Pd-based bimetallic nanoparticles are known to exhibit efficient catalytic properties[21,22], for example, Pd-shell/Pt-core nanoparticles show enhanced electro-catalytic activity[23,24] and it is applicable for fuel cells. In the following, the structural change during synthesis is first observed experimentally, then the formation of bimetallic nanoparticles is simulated by the molecular dynamics (MD) analysis, and the formation process is discussed from the comparison between the experimental and simulated results.

II. EXPERIMENTAL

PdAu, PdAg, and PdPt nanoparticles were fabricated on Al_2O_3 (0001) substrate by co-sputtering. Two RF-magnetron sputtering cathodes are equipped with the sputtering chamber for Pd and another metal, and composition ratio was controlled by changing the input power for the cathodes between 6 W and 35 W, changing the deposition rates between 0.001 nm/s and 0.043 nm/s. Background pressure was less than 4.0×10^{-4} Pa, and Ar pressure during the sputtering was 0.8 Pa.

The formation process was monitored using the resistive spectroscopy[25]. A lithium niobate oscillator, measuring $2.5 \times 1.7 \times 0.2$ mm^3, was placed under the substrate, and the resonant spectrum around the 1.86-MHz resonant mode was repeatedly measured using the line antennas and network analyzer. In previous work[25], we observed that the resonant peak temporarily broadened as the nanoparticles grew and contacted each other on the top surface of the substrate. The vibrating lithium niobate generates the electric field near the substrate surface, and it causes the electrical current flow in the deposited metals. When isolated nanoparticles are formed on the substrate, the surface resistance is significantly high, and energy loss by Joule heating barely occurs. As the nanoparticles grow and the gap distance becomes smaller, the resistance decreases and the current is increased, in which the energy loss becomes larger. After the nanoparticles contact each other and a continuous film is formed, the resistance becomes significantly small, and the energy loss becomes smaller. Therefore, by identifying the timing when the full width at half maximum (FWHM) of the peak is maximum, the transition from isolated nanoparticles to connected nanoparticles is detected. Figure 1(a) shows the resonant spectra measured during the co-sputtering of Pd

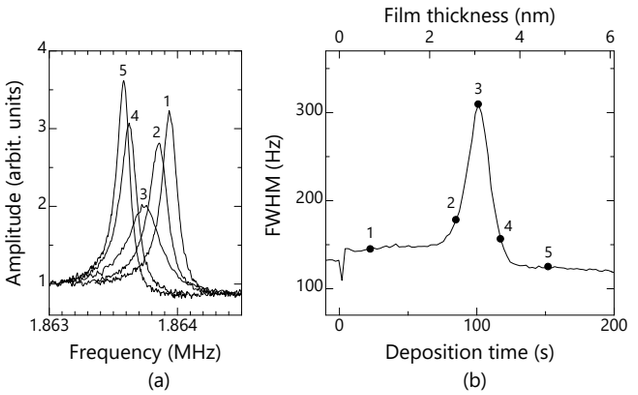

FIG. 1. (a) Representative resonant spectra measured during co-sputtering of Pd and Au and (b) the corresponding FWHM change. Individual points 1-5 in (b) denote the timings at which the corresponding resonant spectra in (a) were obtained.

and Au, and Fig. 1(b) shows the corresponding FWHM change. It is clearly observed that the resonant peak is temporarily broadened, and the FWHM shows the maximum around 100 s, indicating the contact between nanoparticles. The resistive spectroscopy has previously been used for fabricating nanoparticles with nanogaps[26,27]. However, in our previous work[17], it was demonstrated that this method is applicable to investigate structural evolution of core-shell nanoparticles fabricated by sequential sputtering. In this study, it is applied to the co-sputtered nanoparticles to investigate what kind of growth process and internal structure occurs during the fabrication.

The internal structure of nanoparticles is evaluated from the FWHM change. When alloy nanoparticles are synthesized on a substrate, their shape changes depending on their surface energy; as the surface energy increases, the contact angle with substrate increases and it makes nanoparticles spherical. Because the surface energy changes depending on the composition on the surface, evaluating the shape of the nanoparticles would identify the surface composition, which makes it possible to estimate the internal structure of the nanoparticles. However, it is not straightforward to evaluate the shape during sputtering. To overcome this difficulty, we identify the timing of the transition from isolated to connected nanoparticles, because the timing should reflect the nanoparticle shape; as the contact angle decreases, the nanoparticles tend to grow along the substrate surface and contact each other earlier. In this study, we measure the change in FWHM for co-sputtered bimetallic nanoparticles. The results are compared with those measured for sequentially sputtered core-

shell nanoparticles in our previous study[17], and the formation dynamics of co-sputtered alloy nanoparticles are discussed.

III. FWHM-PEAK BASED STRUCTURAL CHARACTERIZATION

Figure 2(a) shows the FWHM changes for the co-sputtered PdAu nanoparticles. A single peak is observed in all nanoparticles, and the peak appears later as the Au fraction increases. The thickness of the nanoparticles at which the FWHM appears was deduced from the deposition rate and it is summarized in Fig. 2(b). The results for sequentially sputtered nanoparticles[17], denoted by B/A, are also shown in Fig. 2; metal B was sputtered after metal A was sputtered. The Au fraction of the nanoparticles denotes the value at the FWHM peak. When the Au fraction was zero (pure Pd), the FWHM peak appeared at a thickness of about 2 nm. The value was almost unchanged at Au fraction of 0-0.5. The thickness increased at Au fraction of 0.7-10, and it became about 4 nm for Au nanoparticles. Similar behavior was observed for Au/Pd nanoparticles, which were synthesized by sputtering Pd followed by Au and Au-shell/Pd-core structure was formed. This similarity indicates that the formation process of co-sputtered PdAu nanoparticles is similar to that of Au/Pd nanoparticles and an Au-shell/Pd-core structure is formed. Considering that the surface energy of Au is lower than that of Pd[28], the segregation of Au on the nanoparticle surface during the co-sputtering is reasonable. In contrast, sequentially sputtered Pd/Au nanoparticles show different behavior; the FWHM peak appeared significantly later than the co-sputtered and Au/Pd nanoparticles. In Pd/Au nanoparticles, interdiffusion occurs during the sputtering of Au due to the high diffusivity of Au atoms, and it causes formation of spherical nanoparticles and segregation of Au are accompanied with it.[17] Such restructuring reduces the growth rate of nanoparticles in the in-plane direction; closure of the gap distances is therefore slow, resulting in a delayed FWHM peak. Such a delayed peak was not observed in the co-sputtered nanoparticles, and their internal structure is different from that of the Pd/Au nanoparticles.

Figure 3(a) shows the results for co-sputtered PdAg nanoparticles. Results for sequentially sputtered Ag/Pd and Pd/Ag nanoparticles[17] are also shown. While a single FWHM peak was observed for the PdAg and Ag/Pd nanoparticles, two peaks were observed for the Pd/Ag nanoparticle. The Pd/Ag nanoparticle was fabricated by changing the deposition

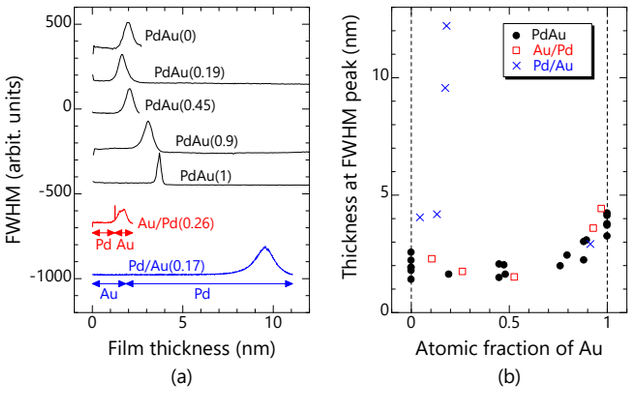

FIG. 2. FWHM change during sputtering for Pd-Au system. (a) Measured FWHM change during the sputtering. The number in parentheses are the atomic fraction of Au at the FWHM peak. (b) Relationship between thickness and atomic fraction of Au at FWHM peak. Experimental results for Pd/Au and Au/Pd nanoparticles are adapted with permission from Phys. Rev. B 105, 125401 (2022). Copylighted by the American Physical Society.

metal from Ag to Pd at a certain moment where nanoparticles were still isolated. Then, Ag nanoparticles were covered with Pd, and gaps between nanoparticles become temporarily wider, because the surface energy of Pd is higher than that of Ag[28], and it increases the contact angle with substrate, making nanoparticles spherical. After this, the gaps between nanoparticles restart to become narrower, and the second peak indicates the timing at which nanoparticles contact. In Pd/Ag nanoparticles, restructuring that was observed in Pd/Au nanoparticles does not occur, and morphological change in Pd/Ag nanoparticles is different from that in Pd/Au nanoparticles.[17] Figure 3(b) shows the thickness at which the FHWM peak appears. Regarding the PdAg nanoparticles, the thickness is unchanged at Ag fraction of 0-0.2. Around Ag fraction of 0.9, the thickness becomes larger, but it is still smaller than that for Ag nanoparticles. This result indicates that structure of PdAg nanoparticles is similar to that for Pd nanoparticles rather than that for Ag nanoparticles. Compared to the sequentially sputtered nanoparticles, the plots for the PdAg nanoparticles appear close to that for the Ag/Pd nanoparticle, rather than those for the Pd/Ag nanoparticles. This result indicates that an Ag-shell/Pd-core structure is formed in PdAg nanoparticles, which is explained by the lower surface energy of Ag than that of Pd.

For PdPt, Pd/Pt, and Pt/Pd nanoparticles, a single FWHM peak was observed as shown in Fig. 4(a). As seen in Fig. 4(b), the FWHM peak appeared around 1 nm regardless

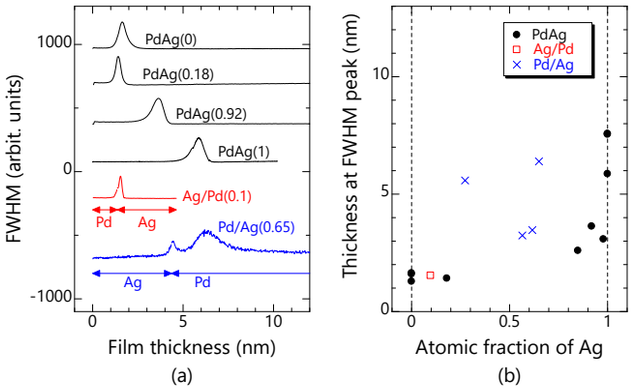

FIG. 3. FWHM change during sputtering for Pd-Ag system. (a) Measured FWHM change during the sputtering. The number in parentheses are the atomic fraction of Ag at the FWHM peak. (b) Relationship between thickness and atomic fraction of Ag at FWHM peak. Experimental results for Pd/Ag and Ag/Pd nanoparticles are adapted with permission from Phys. Rev. B 105, 125401 (2022). Copylighted by the American Physical Society.

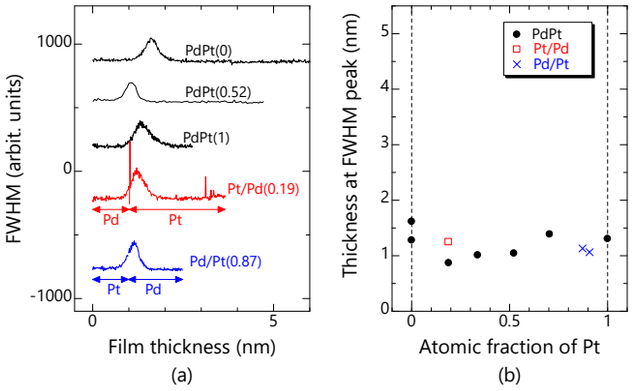

FIG. 4. FWHM change during sputtering for Pd-Pt system. (a) Measured FWHM change during the sputtering. The number in parentheses are the atomic fraction of Pt at the FWHM peak. (b) Relationship between thickness and atomic fraction of Pt at FWHM peak. Experimental results for Pd/Pt and Pt/Pd nanoparticles are adapted with permission from Phys. Rev. B 105, 125401 (2022). Copylighted by the American Physical Society.

of the Pt fraction and the fabrication methods (co-sputtering or sequential sputtering). Considering that the surface energy of Pd is lower than that of Pt[28], the formation of Pd-shell/Pt-core structure was expected. However, no significant difference was observed in the experimental results, and the internal structure could not be deduced.

IV. MOLECULAR DYNAMICS SIMULATION

From the experiments, it was expected that a metal with lower surface energy tend to appear on the surface of co-sputtered nanoparticles, and the morphology of the alloy nanoparticles is similar to that of the core metal. To confirm validity of this interpretation, formation process of the nanoparticles by co-sputtering was simulated by the MD simulation. In Cartesian coordinate system X–Y–Z, X × Y = 9.5 nm × 11.0 nm substrate atomic model was prepared. The substrate was considered as face centered cubic (111) Al atomic layers to simplify the model, and X and Y directions were set as $[11\bar{2}]$ and $[1\bar{1}0]$, respectively. Periodic boundary condition was employed for X and Y, and the vacuum was set along Z direction to mimic the surface of substrate. MD simulation was implemented using this substrate model and to mimic the sputtering process, additional atoms (Pd, Au, Ag and Pt) with random Z direction velocity at the range from -0.01 to -0.02 nm/ps were inserted at the random position with 2.0 to 3.0 nm height from the surface of substrate with the insertion rate 1 atom/ps during MD simulation. Atomic fraction of Au, Ag, and Pt was set to be 0.0, 0.1, 0.3, 0.5, 0.7, 0.9, and 1.0 for PdAu, PdAg, and PdPt co-sputtering simulations, respectively. Shan *et al*. embedded atom method (EAM) potential[29,30] was used as interaction potential between Pd–Pd, Pd–Au, and Au–Au atoms for PdAu co-sputtering simulation. Hale *et al*. EAM potential[31] was used as interaction potential between Pd–Pd, Pd–Ag, and Ag–Ag atoms for PdAg co-sputtering simulation. Zhou *et al*. EAM potential[32] was used as interaction potential between Pd–Pd, Pd–Pt, and Pt–Pt atoms for PdPt co-sputtering simulation. We confirmed (111) surface energy of Au, Ag and Pt are 1.68, 7.16 eV/nm^2 lower and 2.06 eV/nm^2 higher than that of Pd for each potentials, which is qualitatively consistent with the previous study[28]. Mimicking the van der Waals force between the substrate atom and sputtered atoms, Al–Al and Al–(sputtered atom) interactions were described using a conventional Lennard–Jones form,

$$E(r_{ij}) = 4\varepsilon \left[\left(\frac{\sigma}{r_{ij}} \right)^{12} - \left(\frac{\sigma}{r_{ij}} \right)^{6} \right]. \tag{1}$$

r_{ij} is the distance between i and j atoms. From parameter study, the values of σ and ε for Al–Al and Al–(sputtered atom) were determined as Table I as MD simulation can reproduce the timing of the FWHM peak measured in the experiments. For example, the experimental result that the FHWM peak of Pd appears earlier than that of Au indicates that the covering

TABLE I. The values of Lennard–Jones potential parameters σ and ε for Al–Al and Al–(sputtered atom) interaction. The unit of σ and ε are eV and nm, respectively.

	ε	σ
Al–Al	0.507	0.246
Al–Pd	0.1	0.246
Al–Au	0.06	0.246
Al–Ag	0.05	0.246
Al–Pt	0.4	0.246

of the substrate surface by Pd progresses faster than that by Au. The parameters were determined to reproduce this difference in the progress of the surface coverage. Note for Al–Al interaction, we refered Filippova *et al.*'s values[33] and adjusted them as the lattice constant is consistent with that of alumina, 0.475 nm. LAMMPS[34] code is used and MD co-sputtering simulation was implemented for 5 ns at constant temperature 300 K with time step 1 fs. Representative animations of nanoparticles growth are shown in supplementary material.

Figure 5 shows the snapshots at 1.5 ns, where nanoparticles are isolated on substrate. In PdAu nanoparticles, Au atoms tend to appear on the nanoparticle surfaces, and nanoparticles are almost covered with Au at Au fraction of 0.7. The Au segregation on the surface agrees with that expected from the experimental results. Surface coverage of substrate by nanoparticles was also evaluated. Figure 6 shows the surface coverage at 1.5 ns. For PdAu nanoparticles, surface coverage gradually decreased as Au fraction increased, and between 0.9 and 1.0 the coverage decreased significantly. Regarding the number of nanoparticles, 8-10 nanoparticles are formed at 0.0-0.5, and it decreases at 0.7-1.0, which indicates that the shape of nanoparticles tends to be similar to that of Pd nanoparticles even at Au fraction of 0.5. Similar behaviors were observed at 3.0 ns, where some nanoparticles start to contact (snapshots are shown in supplementary material). From these results, it is expected that formation dynamics of PdAu nanoparticles is similar to that of Pd nanoparticles, even when the surface of the nanoparticles is covered with Au.

Similar behaviors were observed in PdAg nanoparticles. Nanoparticles tended to be

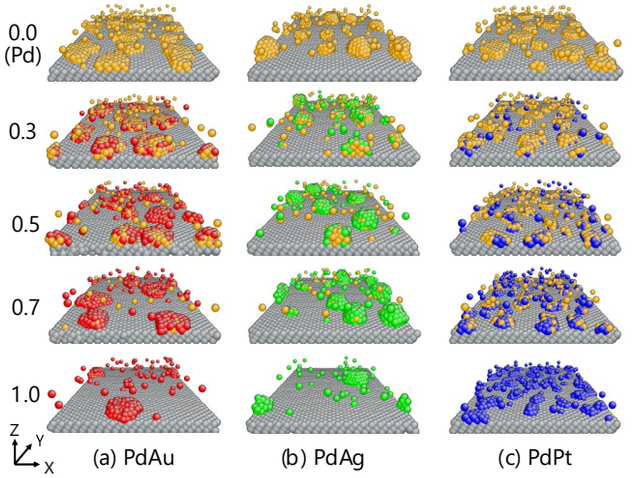

FIG. 5. MD simulation results for co-sputtering of (a) PdAu, (b) PdAg, and (c) PdPt. Images were obtained at 1.5 ns. Atomic fractions of Au, Ag, and Pt are 0.0, 0.3, 0.5, 0.7, and 1.0 from top to bottom. Yellow, red, green, and blue particles denote Pd, Au, Ag, and Pt atoms, respectively.

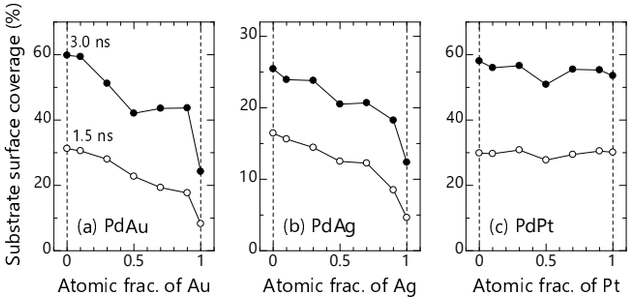

FIG. 6. Surface coverage of substrate at 1.5 and 3.0 ns obtained by the MD simulations for co-sputtering of (a) PdAu, (b) PdAg, and (c) PdPt.

covered with Ag rather than Pd (Fig. 5(b)). The surface coverage of the substrate decreased as the Ag fraction increased, and it decreased significantly between 0.9 and 1.0 of Ag fraction (Fig. 6(b)). A few nanoparticles were formed in Pd and PdAg nanoparticles though only two nanoparticles were formed in Ag nanoparticles. These results expect that the formation dynamics of PdAg nanoparticles is similar to that of Pd rather than that of Ag.

In PdPt nanoparticles, Pd tended to appear on nanoparticle surface, and the number of nanoparticles increased as the Pt fraction increased (Fig. 5(c)). The surface coverage of the substrate was almost independent of Pt fraction as shown in Fig. 6(c), and the behavior is similar to that experimentally observed in Fig. 4(b). In the experiments, formation of

core-shell structure was not confirmed, but the Pd-shell/Pt-core structure was observed in the MD simulations.

From the experimental and MD simulation results, it was confirmed that core-shell nanoparticles are formed by co-sputtering and a metal with lower surface energy tends to appear on the nanoparticle surface; Au, Ag, and Pd appear on the surface of PdAu, PdAg, and PdPt nanoparticles, respectively. Surface energy of nanoparticles depends on the composition and crystallographic orientation appearing on the nanoparticle surface. In Fig. 5, (111) planes tend to appear on the nanoparticle surface, and the surface energy of (111) plane is expected to play the dominant role. Although under certain conditions the electronic energy also affects the total energy[35] and changes the shape of the nanoparticles, this is not the case. Considering that the contact angle of nanoparticles with substrate changes depending on the surface energy of nanoparticles, it was expected that the shape of the nanoparticles would be similar to that made of the metal appearing on the nanoparticle surface, e.g. Au in PdAu nanoparticles. However, the shape tended to be similar to that made of the core metal, even when the atomic fraction of shell metal is higher than that of core metal and surface of the nanoparticles is covered with the shell metal. These results suggest that the formation process of alloy nanoparticles is as follows; the core nanoparticles are formed predominantly on the substrate, and the shell metal diffuses onto the nanoparticle surface.

The segregation in alloy nanoparticles can be expected from the surface energies of the constituting metals, but it is difficult to predict the formation process of nanoparticles by the conventional experimental and analytical methods. In this study, we demonstrated that the formation process can be investigated by performing the in-situ observation of the morphological change during the co-sputtering.

V. CONCLUSIONS

In summary, formation dynamics of Pd-based bimetallic nanoparticles synthesized by the co-sputtering was experimentally and theoretically investigated by detecting the timing at which nanoparticles contact on substrate and by the MD simulation. From both the experimental and MD simulation results, it was confirmed that core-shell nanoparticles were formed by co-sputtering. In addition, we observed that the formation process highly

depends on that of core nanoparticles even when the atomic fraction of shell metal is higher and the nanoparticle surface is covered with the shell metal.

SUPPLEMENTARY MATERIAL

See supplementary material for the MD simulation results; animations of nanoparticle growth, snapshots (morphology of nanoparticles) at 3.0 ns, and changes in the surface coverage of substrate with time.

ACKNOWLEDGMENTS

This research was partially supported by JSPS KAKENHI Grants No. 18H01883 and No. 20K21145.

AUTHOR DECLARATIONS

Conflict of Interest

The authors have no conflicts to disclose.

Author Contributions

Nobutomo Nakamura Conceptualization (lead); Formal Analysis (equal); Funding Acquisition (lead); Investigation (supporting); Methodology (lead); Supervision (lead); Writing/Original Draft Preparation (lead); Writing/Review & Editing (equal) **Koji Matsuura** Investigation (lead); Formal Analysis (equal); Writing/Review & Editing (equal) **Akio Ishii** Investigation (supporting); Formal Analysis (equal); Software (lead); Writing/Original Draft Preparation (supporting); Writing/Review & Editing (equal)

DATA AVAILABILITY

The data that support the findings of this study are available from the corresponding author upon reasonable request.

REFERENCES

[1]N. Toshima and T. Yonezawa, New J. Chem. **22**, 1179 (1998)

[2]R. Ferrando, J. Jellinek, and R. L. Hohnston, Chem. Rev. **108**, 845 (2008).

[3]L. L. Wang and D. D. Johnson, J. Am. Chem. Soc. **131**, 14023 (2009).

[4]J. L. Rousset, J. C. Bertolini, and P. Miegge, Phys. Rev. B **53**, 4947 (1996).

[5]R. Marchal, A. Genest, S. Krüger, and N. Rösch, J. Phys. Chem. C **117**, 21810 (2013).

[6]K. Luo, T. Wei, C.-W. Yi, S. Axnanda, and D. W. Goodman, J. Phys. Chem. B **109**, 23517 (2005).

[7]A. R. Haire, J. Gustafson, A. G. Trant, T. E. Jones, T. C. Q. Noakes, P. Bailey, C. J. Baddeley, Surf. Sci. **605**, 214 (2011).

[8]J. W. Hu, Y. Zhang, J. F. Li, Z. Liu, B. Ren, S. G. Sun, Z. Q. Tian, and T. Lian, Chem. Phys. Lett. **408**, 354 (2005).

[9]K. Rajoua, L. Baklouti, and F. Favier, J. Phys. Chem. C **119**, 10130 (2015).

[10]Y. W. Lee, M. Kim, Z. H. Kim, and S. W. Han, J. Am. Chem. Soc. **131**, 17036 (2009).

[11]M. Hirano, K. Enokida, K. Okazaki, S. Kuwabata, H. Yoshida, and T. Torimoto, Phys. Chem. Chem. Phys. **15**, 7286 (2013).

[12]S. M. Sadeghi, A. Hatef, A. Nejat, Q. Campbell, and M. Neunier, J. Appl. Phys. **115** 134315 (2014).

[13]S. Verma, B. T. Rao, A. P. Detty, V. Ganesan, D. M. Phase, S. K. Rai, A. Bose, S. C. Joshi, and L. M. Kukreja, J. Appl. Phys. **117** 133105 (2015).

[14]X. Guo, P. Brault, G. Zhi, A. Caillard, G. Jin, and X. Guo, J. Phys. Chem. C **115**, 24164 (2011).

[15]Y. Bao, H. Calderon, and K. M. Krishnan, J. Phys. Chem. C **111**, 1941 (2007).

[16]J. T. McKeown, Y. Wu, J. D. Fowlkes, P. D. Rack, and G. H. Campbell, Adv. Mater. **27**, 1060 (2015).

[17]N. Nakamura, K. Matsuura, A. Ishii, and H. Ogi, Phys. Rev. B **105**, 125401 (2022).

[18]G. Randnóczi, E. Bokányi, Z. Erdélyi, and F. Misják, Acta. Mater. **123**, 82 (2017).

[19]R. Cai, P. R. Ellis, J. Yin, J. Liu, C. M. Brown, R. Griffin, G. Chang, D. Yang, J. Ren, K. Cooke, P. T. Bishop, W. Theis, and R. E. Palmer, Small **14**, 1703734 (2018).

[20]M. T. Nguyenm H. Zhang, L. Deng, T. Tokunaga, and T. Yonezawa, Langmuir **33**, 12389 (2017).

[21]R. G. Chaudhuri and S. Paria, Chem. Rev. **112**, 2373-2433 (2012).

[22]K. Tedsree, T. Li, S. Jones, C. W. A. Chan, K. M. K. Yu, P. A. Bagot, E. A. Marquis, G. D. Smith, and S. C. E. Tsang, Nat. Nanotechnol. **6**, 302 (2011).

[23]Y. Li, Z. Wei, C. Chiu, L. Ruan, W. Yang, Y. Yang, R. E. Palmer, and Y. Huang, Nanoscale **4** (2012) 845.

[24]A. Higareda, G. Rosas, R. Pérez, and R. Esparza, Chem. Nano Mat. **7** (2021) 958.

[25]N. Nakamura and H. Ogi, Appl. Phys. Lett. **111**, 101902 (2017).

[26]N. Nakamura, T. Ueno, and H. Ogi, Appl. Phys. Lett. **114**, 201901 (2019).

[27]N. Nakamura, T. Ueno, and H. Ogi, J. Appl. Phys. **126**, 225104 (2019).

[28]W. R. Tyson and W. A. W. Miller, Surf. Sci. **62**, 267 (1977).

[29]B. Shan, L. Wang, S. Yang, J. Hyun, N. Kapur, Y. Zhao, J. B. Nicholas, and K. Cho, Phys. Rev. B **80**, 035404 (2009).

[30]B. Shan, L. Wang, S. Yang, J. Hyun, N. Kapur, Y. Zhao, J. B. Nicholas, and K. Cho, Phys. Rev. B **89**, 159903 (2014).

[31]L. M. Hale, B. M. Wong, J. A. Zimmerman, and X. W. Zhou, Modell. Simul. Mater. Sci. Eng. **21**, 045005 (2013).

[32]X. W. Zhou, R. A. Johnson, and H. N. Wadley, Phys. Rev. B **69**, 144113 (2004).

[33]V. P. Filippova, S. A. Kunavin, and M. S. Pugachev, Inorg. Mater. Appl. Res. **6**, 1 (2015).

[34]S. Plimpton, J. Comput. Phys. **117**, 1 (1995).

[35]T. E. Kidd, P. Kruckenbert, C. Gorgen, P. V. Lukashev, and A. J. Strollenwerk, J. Appl. Phys. **132** (2022) 245301.

AIP Publishing

Journal of Applied Physics

PLEASE CITE THIS ARTICLE AS DOI: 10.1063/5.0149492

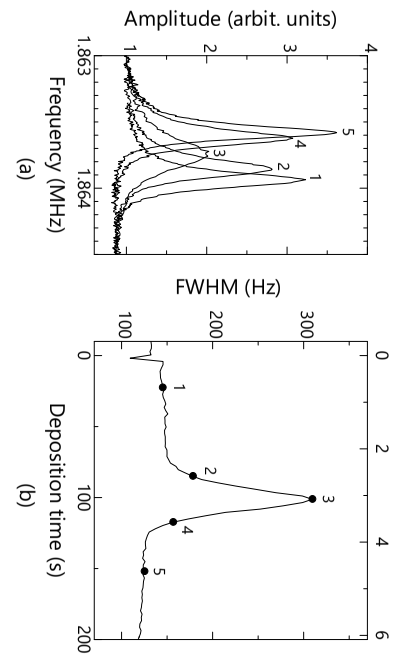

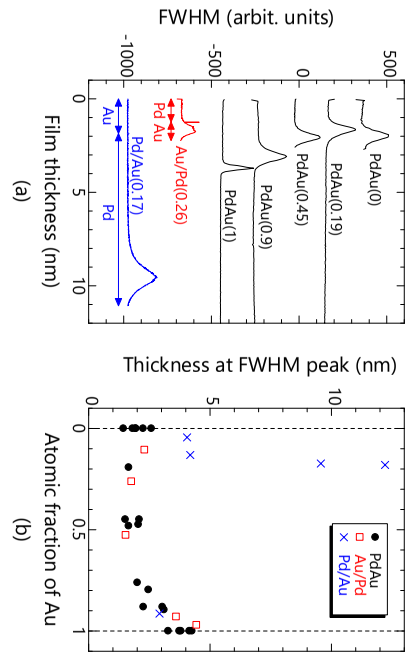

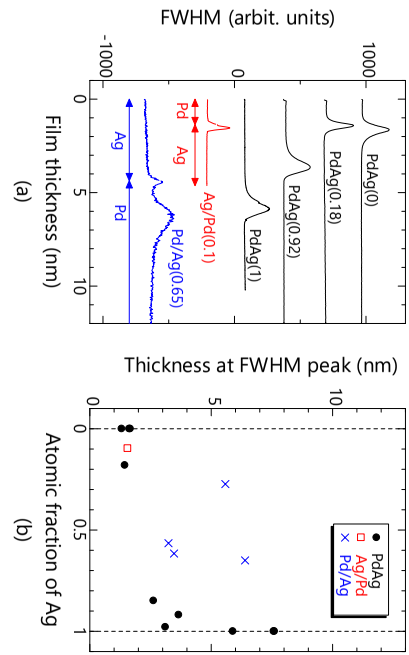

AIP Publishing

Journal of Applied Physics

ACCEPTED MANUSCRIPT

PLEASE CITE THIS ARTICLE AS DOI: 10.1063/5.0149492

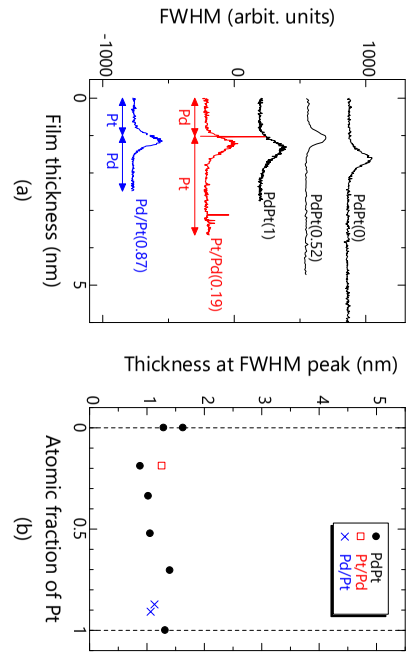

AIP Publishing

Journal of Applied Physics

ACCEPTED MANUSCRIPT

This is the author's peer reviewed, accepted manuscript. However, the online version of record will be different from this version once it has been copyedited and typeset.
PLEASE CITE THIS ARTICLE AS DOI: 10.1063/5.0149492

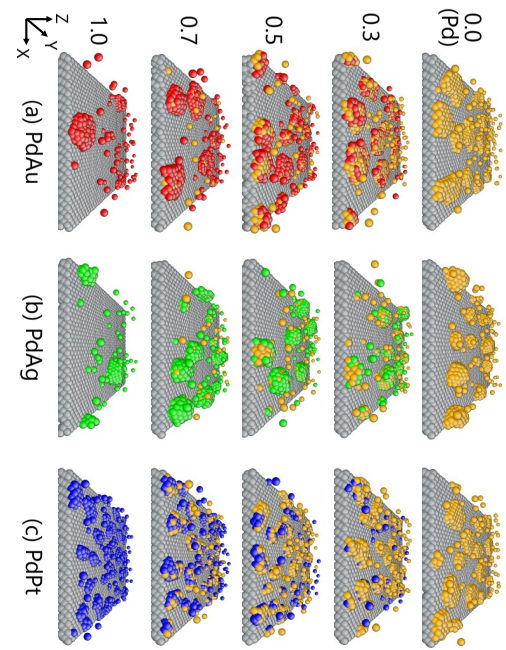

AIP Publishing

Journal of Applied Physics

ACCEPTED MANUSCRIPT

This is the author's peer reviewed, accepted manuscript. However, the online version of record will be different from this version once it has been copyedited and typeset.
PLEASE CITE THIS ARTICLE AS DOI: 10.1063/5.0149492